

Impact of Ferroquine on the Solubilization of Artefenomel (OZ439) during *in Vitro* Lipolysis in Milk and Implications for Oral Combination Therapy for Malaria

Malinda Salim,[†] Jamal Khan,[†] Gisela Ramirez,[†] Mubtasim Murshed,[†] Andrew J. Clulow,[†] Adrian Hawley,[‡] Hanu Ramachandruni,[§] Stephane Beilles,^{||} and Ben J. Boyd^{*,†,⊥}

[†]Drug Delivery, Disposition and Dynamics, Monash Institute of Pharmaceutical Sciences, Monash University (Parkville Campus), 381 Royal Parade, Parkville, VIC 3052, Australia

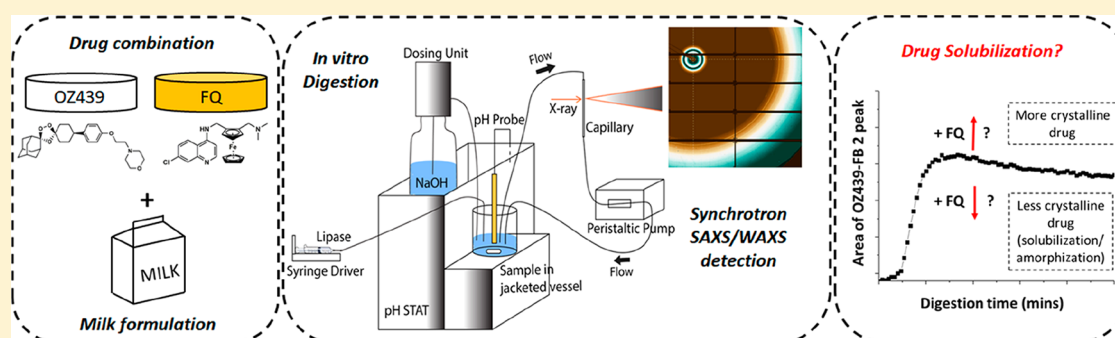
[‡]SAXS/WAXS Beamline, Australian Synchrotron, ANSTO, 800 Blackburn Road, Clayton, VIC 3169, Australia

[§]Medicines for Malaria Venture, 20, Route de Pré-Bois, 1215 Geneva 15, Switzerland

^{||}Sanofi R&D, 371 Rue du Professeur Blayac, 34080 Montpellier, France

[⊥]ARC Centre of Excellence in Convergent Bio-Nano Science and Technology, Monash Institute of Pharmaceutical Sciences, Monash University (Parkville Campus), 381 Royal Parade, Parkville, VIC 3052, Australia

Supporting Information



ABSTRACT: Milk is an attractive lipid-based formulation for the delivery of poorly water-soluble drugs to pediatric populations. We recently observed that solubilization of artefenomel (OZ439) during *in vitro* intestinal lipolysis was driven by digestion of triglycerides in full-cream bovine milk, reflecting the ability of milk to act as an enabling formulation in the clinic. However, when OZ439 was co-administered with a second antimalarial drug, ferroquine (FQ) the exposure of OZ439 was reduced. The current study therefore aimed to understand the impact of the presence of FQ on the solubilization of OZ439 in milk during *in vitro* intestinal digestion. Synchrotron small-angle X-ray scattering was used for *in situ* monitoring of drug solubilization (inferred via decreases in the intensity of drug diffraction peaks) and polymorphic transformations that occurred during the course of digestion. Quantification of the amount of each drug solubilized over time and analysis of their distributions across the separated phases of digested milk were determined using high-performance liquid chromatography. The results show that FQ reduced the solubilization of OZ439 during milk digestion, which may be due to competitive binding of FQ to the digested milk products. Interactions between the protonated FQ-H⁺ and ionized liberated free fatty acids resulted in the formation of amorphous salts, which removes the low-energy crystalline state as a barrier to dissolution of FQ, while inhibiting the solubilization of OZ439. We conclude that although milk could enhance the solubilization of poorly water-soluble OZ439 during *in vitro* digestion principally due to the formation of fatty acids, the solubilization efficiency was reduced by the presence of FQ by competition for the available fatty acids. Assessment of the solubilization of both drugs during digestion of fixed-dose combination lipid formulations (such as milk) is important and may rationalize changes in bioavailability when compared to that of the individual drugs in the same formulation.

KEYWORDS: antimalarial, poorly water-soluble drug, milk, lipid-based formulation, *in vitro* digestion, solubilization, polymorphism, X-ray scattering

1. INTRODUCTION

Lipid-based formulations can improve the solubilization of poorly water-soluble drugs in the gastrointestinal (GI) tract and eliminate the rate-limiting dissolution step in intestinal

Received: December 27, 2018

Revised: February 12, 2019

Accepted: February 19, 2019

Published: March 4, 2019

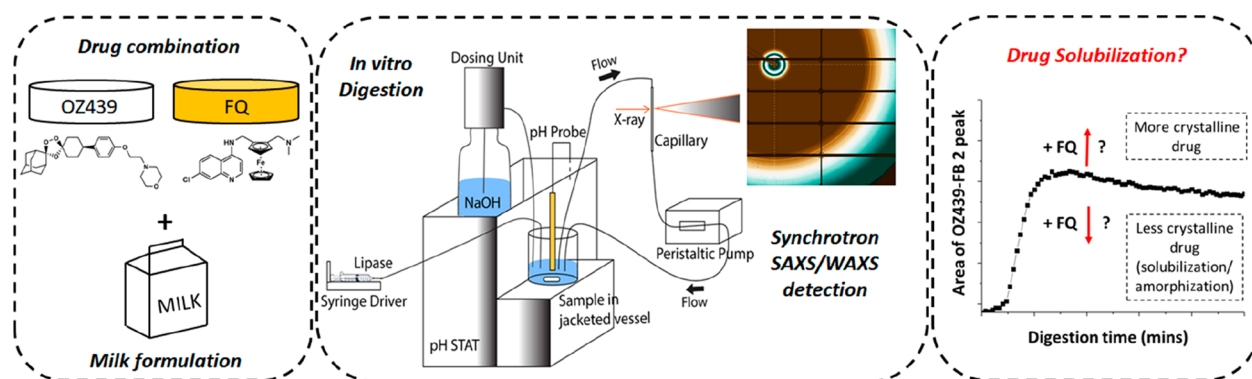


Figure 1. Schematic of the major aspects of this study. Left panel: Chemical structures of the free bases of OZ439 and ferroquine (FQ). Middle panel: pH stat digestion system coupled to a capillary for *in situ* time-resolved X-ray scattering. Right panel: typical profile for residual crystalline drug (OZ439-FB form 2 in this case) during the digestion of milk-based formulations.

absorption.¹ Many poorly water-soluble drugs exhibit strong food effects,^{1,2} and co-administration of full-cream milk with artefenomel (OZ439, $\log P \approx 5.4$ predicted using Chemicalize developed by ChemAxon), for example, leads to an improved bioavailability in patients with uncomplicated malaria.^{3,4} Milk has been demonstrated to be an effective drug delivery system when digestion is considered as an essential factor in understanding its performance as a formulation.⁵ In our previous work, we attempted to understand the solubilization behavior of OZ439 in milk during *in vitro* digestion.⁶ The mesylate salt of OZ439 is the preferred salt form that has been prepared commercially; however, upon exposure of a solution of the mesylate salt in water to low-pH chloride solutions mimicking the gastric environment, the crystalline hydrochloride salt immediately precipitated. Subsequent exposure to neutral-pH simulated intestinal conditions caused transformation to the free base (OZ439-FB form 1).^{6,7} The free base form 1 then underwent a polymorphic transformation to the stable crystalline OZ439-FB form 2 during digestion in milk, which was subsequently partially solubilized into the digested milk. However, the bioavailability of OZ439 when given with milk in the clinic was sufficient to elicit its therapeutic effect.⁸

Since the use of two antimalarial drugs with different mechanisms of action is recommended to reduce the potential resistance of malaria parasites,^{4,9} a combination of OZ439 and ferroquine (FQ, $\log P \approx 5.1$)¹⁰ has been recently supported under a program by Medicines for Malaria Venture (MMV) in partnership with Sanofi. The chemical structures of OZ439 and FQ are presented in Figure 1. OZ439 has been reported to have a mechanism of action similar to that of artemisinin, where cleavage of the endoperoxide bond by Fe^{2+} and heme released during hemoglobin digestion could generate free radicals that alkylate key parasitic proteins.¹¹ Meanwhile, the basic 4-aminoquinoline moiety in FQ could accumulate in the acidic digestive vacuole of the parasite, thus preventing the formation of hemozoin, which leads to the death of the parasite.¹⁰ The ferrocenyl core in FQ could also contribute to the antiplasmodial activity by redox cycling (between Fe^{3+} and Fe^{2+}), which generates toxic free radicals.¹² The efficacy of this combinatorial drug as a single-dose therapy for uncomplicated malaria is currently under phase 2b clinical trial.¹³ However, when the drugs were administered in a combination drug dose, a reduction in exposure to OZ439 in the presence of FQ was discovered. Hence, the current study aims to elucidate whether a physico-chemical mechanism may be responsible.

Therefore, the effects of milk digestion on the solubilization of FQ were established to complement our previous work on OZ439 and then extended to consider the quantitative solubilization of both drugs when combined during digestion of the milk formulation *in vitro*. As illustrated schematically in Figure 1, synchrotron small-angle X-ray scattering (SAXS) was used to monitor simultaneously the solubilization of the drugs and the changes in the polymorphic state of the two drugs in real time during digestion. This method has been successfully used to provide time-resolved measurements in similar systems.^{14,15} High-performance liquid chromatography (HPLC) was used to quantify the distributions of OZ439 and FQ in the digested milk phases.

2. EXPERIMENTAL SECTION

2.1. Materials and Chemicals. The free base form of the FQ active pharmaceutical ingredient (FQ API, SSR97193) and FQ granules that contain 50 wt% FQ API were supplied by Sanofi (Montpellier, France). OZ439 mesylate salt was provided by MMV. Full-cream bovine milk (3.8 wt% fat) was purchased from a Coles supermarket (Brunswick or Mt. Waverley, Victoria, Australia). The complete nutritional information has been supplied previously for this brand of full-fat milk.⁵ Trizma maleate (reagent grade), casein from bovine milk (technical grade), dimethyl sulfoxide (DMSO, $\geq 99.5\%$), and 4-bromophenylboronic acid (4-BPBA, $>95\%$) were purchased from Sigma-Aldrich (St. Louis, Missouri). Trifluoroacetic acid (TFA, $\geq 99.9\%$) was purchased from VWR (HiPerSolv CHROMANORM for HPLC, Australia). Calcium chloride dihydrate ($>99\%$) and sodium hydroxide pellets (min. 97%) were purchased from Ajax Finechem (Seven Hills, New South Wales, Australia). Sodium chloride ($>99\%$) was purchased from Chem Supply (Gillman, South Australia, Australia). Sodium azide ($\geq 99\%$) was purchased from Fluka (Sigma-Aldrich, St. Louis, Missouri). Acetonitrile (liquid chromatography grade) was purchased from Merck (Darmstadt, Germany). USP-grade pancreatin extract was purchased from Southern Biologicals (Nunawading, Victoria, Australia). Unless otherwise stated, all chemicals were used as received without further purification, and water was sourced from Millipore Milli-Q water purification systems at the point of use.

2.2. In Vitro Lipolysis of FQ and OZ439 + FQ Mixtures in Milk. Digestion of milk containing the antimalarial drugs OZ439 and FQ was performed using a pH-stat apparatus (Metrohm 902 STAT titration system) equipped with Tiamo

version 2.5 software. Dosages of the drugs were selected based on the equivalent amount of 800 mg of OZ439 free base and 900 mg of FQ free base in 200 mL of fluid to reflect a potential clinical combination. The OZ439 mesylate (99 mg, equivalent to 82 mg of OZ439-FB), FQ granules (186 mg, equivalent to 93 mg of FQ API), or both were mixed and dissolved in 2.75 mL of water containing 0.25 mL of 1 M HCl solution to simulate the gastric pre-treatment step of the drugs. The drug solutions were added to 17.5 mL of full-cream milk or 2× diluted milk (diluted with the tris-maleate buffer described below) in a temperature-controlled glass vessel at 37 °C, and the pH was adjusted to 6.500 ± 0.003 prior to the start of each digestion experiment. The corresponding ratios of OZ439-FB and FQ API to the milk fat were 124 and 140 mg/g, respectively. After the pH was adjusted to 6.500 and the solution was equilibrated for 3 min, the digestion phase was initiated by a remote injection of 2.25 mL of reconstituted lipase suspension. To prepare the lipase suspension, pancreatin was dispersed in water and centrifuged, and the supernatant was freeze-dried to provide a powder form. The freeze-dried powder was then dispersed in digestion buffer (50 mM tris-maleate buffer at pH 6.5 containing 5 mM $\text{CaCl}_2 \cdot 2\text{H}_2\text{O}$, 6 mM NaN_3 and 150 mM NaCl), with a lipase activity of around 700 TBU per mL of digest. NaOH (2 M) solution was titrated into the vessel under software control to maintain the pH of the sample at pH 6.5 during lipolysis, which would otherwise drop due to the liberation of free fatty acids (FFAs) during digestion. The digested samples were subjected to centrifugation at 14462g for 30 min at 25 °C to isolate the pellets for solid-state analysis.

The amount of ionized digestion products released during digestion at pH 6.5 was calculated from the volume of NaOH consumed after subtraction of the control measurement on the same volume of buffer containing no milk fat or protein, and the total amounts of ionized and non-ionized species were determined by back-titration to pH 9.0 at the end of digestion (see Table S1, Supporting Information). The back-titration step was performed by increasing the pH of the final digested sample to 9.0 to completely deprotonate all liberated FFAs. The amount of NaOH added in the back-titration was subtracted from the corresponding values obtained during the back-titration of the control sample (no milk) to account for titration from the pancreatic lipase and the drugs.

2.3. Synchrotron Small-Angle X-ray Scattering (SAXS). **2.3.1. Time-Resolved Flow-Through Configuration.** The pH stat apparatus was interfaced with the SAXS/WAXS beamline at the Australian Synchrotron, part of ANSTO.¹⁶ This setup (Figure 1 central panel) allowed for real-time monitoring of drug solubilization and polymorphic transformations, as well as liquid crystalline structure formation by the self-assembly of milk lipolytic products. Samples were loaded into a thermostatted (37 °C) digestion vessel and were aspirated through a fixed quartz capillary mounted in the synchrotron X-ray beam using a peristaltic pump operating at 10 mL/min. An X-ray beam with a wavelength (λ) of 0.954 Å (photon energy = 13 keV) was used in this study. Sample-to-detector distances of around 1.6 and 0.6 m were used to detect the liquid crystalline structures and the drugs, respectively. These sample-to-detector distances afforded q ranges of $0.01 < q < 0.40$ (1.6 m) and $0.04 < q < 2.00$ (0.6 m) \AA^{-1} , where q is defined as the length of the scattering vector i.e., $(4\pi/\lambda)\sin(2\theta/2)$, where 2θ is the scattering angle. 2D SAXS patterns were recorded using a Pilatus 1 M detector with 5 s

acquisition times and a 15 s delay between measurements (one measurement every 20 s). The 2D data were reduced to scattering functions $I(q)$ versus q by radial integration using the in-house software ScatterBrain Version 2.71.

2.3.2. Equilibrium Static Configuration for Measurements of Solid-State Drug Powders and Pellets. SAXS patterns of the FQ API powder, FQ granules, re-precipitated FQ API (to check for any polymorphic transformation of FQ from gastric to intestinal pH), and the pellets collected after ultracentrifugation of the digested samples were obtained by loading the samples into 1.5 mm outer-diameter glass microcapillaries placed in the X-ray beam. The sample-to-detector distance used was approximately 0.6 m, with an X-ray energy of 13 keV. The re-precipitated FQ API sample was prepared by dissolving 93 mg of FQ API in 2.75 mL of water containing 0.25 mL of 1 M HCl, followed by adjustment of the pH to 6.5.

2.4. Quantification of Drug Solubilization Using High-Performance Liquid Chromatography (HPLC). HPLC was used to quantify the amount of OZ439 and FQ in the colloidal phases during 1 h of *in vitro* digestion. Samples (300 μL) were collected from the digestion vessel at different times during the digestion experiments (0, 2, 5, 10, 30, and 60 min) and transferred to glass vials containing 30 μL of the lipase inhibitor (0.05 M 4-BPBA in methanol).^{6,17} To examine the effect of methanol on the partitioning of OZ439 and FQ in the digested phases, a smaller amount of more concentrated inhibitor solution (3 μL of 0.5 M 4-BPBA in methanol) was also used to inhibit the digestion.

Polycarbonate centrifuge tubes (7 × 20 mm, Beckman Coulter) were loaded with 200 μL of the samples collected at the different time points and centrifuged for 40 min at 329177g at 37 °C using an Optima MAX-TL ultracentrifuge (Beckman Coulter, Indiana, USA) with a TLA-100 rotor. The resulting upper lipid layer and the aqueous phase containing lipid colloidal phases were transferred into separate 2 mL glass vials using a 1 mL syringe and 25-gauge needle. DMSO (800 μL) was added to both the lipid layer and the aqueous phase in their respective 2 mL glass vials. These samples were subsequently diluted with 95:5 v/v mobile phase A:B and analyzed by HPLC. The mobile phase A contained water with 0.1 vol% TFA, and mobile phase B contained acetonitrile with 0.085 vol% TFA. The pellet phases were similarly treated with DMSO and were diluted in 5:95 v/v mobile phase A:B before analysis by HPLC.

The samples (lipid, aqueous, and pellet layers) from the different time points as described above were compared to a standard curve, which was determined using stock solutions of OZ439 (8 mg/mL in DMSO) and FQ API (2 mg/mL in DMSO). The first standard was prepared by adding 250 μL of OZ439 (8 mg/mL in DMSO), 500 μL of FQ API (2 mg/mL in DMSO), 200 μL of digested milk (without the prior addition of any drug), and an additional 50 μL of DMSO. A serial dilution was performed on the above standard, halving the concentration of OZ439 and FQ with each dilution, using a diluent consisting of digested milk and DMSO (1:4 volume ratio), which represented the sample matrix.

The HPLC system consisted of a Shimadzu CBM-20A system controller, an LC-20AD solvent delivery module, an SIL-20A auto-sampler, and a CTO-20A column oven set at 35 °C, coupled to an SPD-20A UV detector (Shimadzu Corporation, Kyoto, Japan). A reverse-phase C_{18} column was used (4.6 × 75 mm², 3.5 μm ; Waters Symmetry,

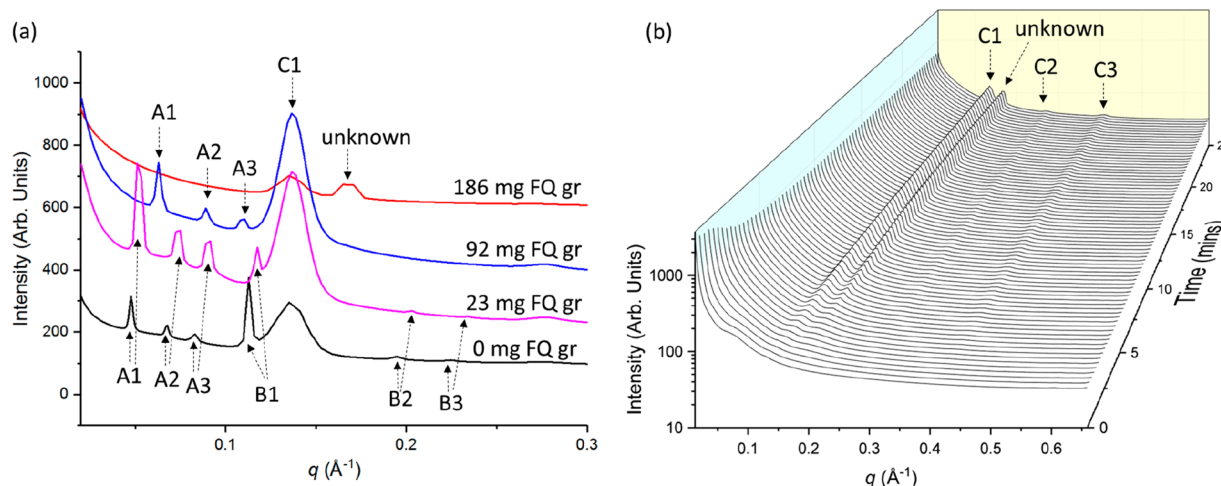


Figure 2. (a) Final X-ray scattering profiles of digested milk in the presence of added FQ granules from 0 mg (milk only), 23 mg, 92 mg and 186 mg after 25 min digestion. The corresponding FB concentrations of the FQ were 12 mg (for 23 mg of FQ granules), 46 mg (for 92 mg of FQ granules), and 93 mg (for 186 mg of FQ granules). A1, A2, and A3 represent the first, second, and third peaks of an $Im3m$ phase with the reciprocal spacing ratios of $\sqrt{2}:\sqrt{4}:\sqrt{6}$, while B1, B2, and B3 represent the peaks of an H_2 phase with the reciprocal spacing ratios of $1:\sqrt{3}:\sqrt{4}$. Peaks of the equidistant $L\alpha$ phase are labeled as C1, C2, and C3. (b) X-ray scattering plot of the time-dependent structure formation for the digestion of milk with 186 mg FQ granules.

Massachusetts, USA), and the UV detector was set to record at 260 nm for the detection of OZ439 and FQ using a binary gradient of mobile phases A and B. The mobile phase gradient used consisted of 5–95% B for 6 min, 95–5% B for 12 s, and 5% B for 5.8 min at 0.5 mL/min flow rate, with an injection volume of 50 μ L. The retention times for OZ439 and FQ were 7.0 and 4.4 min, respectively, using these elution conditions.

2.5. Particle Size Measurements Using Laser Light Scattering. Size distributions by volume of the digested milk particles in the absence and presence of OZ439 and FQ granules during digestion (the digestion methods are described in detail in section 2.3) were obtained using a Mastersizer S laser particle size analyzer equipped with a He-Ne laser (wavelength 633 nm) and a 300-RF lens to detect particles with sizes ranging from 0.05 to 880 μ m. The refractive indices used were 1.46 for milk fat in water and 1.33 for water. The particle density of the milk fat was taken to be 0.92 g/cm³. The digested milk samples were collected at 0 (before lipase injection) and 60 min and were diluted in 50 mL of water in the sample preparation unit to obtain obscurations of between 10 and 15% (typical sample volume = 150–500 μ L).

3. RESULTS

3.1. Effects of OZ439 and FQ on the Digestion and Self-Assembled Lipid Structures in Milk. The X-ray scattering patterns in Figure 2 show that the final structures (after 60 min digestion) formed by the self-assembly of digested milk products were altered when OZ439 and FQ were present in the system. Self-assembled structures were still retained after dosing 42 mg of free base (FB) equivalents of OZ439 (50 mg of the OZ439 mesylate salt), which had lattice parameters similar to those of milk in the absence of drug.¹⁸ In comparison, addition of 46 mg of FQ-FB equivalent (92 mg of FQ granules) caused a shift in the positions of the Bragg peaks characteristic of the inverse bicontinuous cubic phase ($Im3m$) and the disappearance of the Bragg peaks corresponding to the H_2 phase on digestion (Figure 2b). At the recommended clinical dosage of 186 mg of FQ granules per 20.25 mL of fluid, only a small peak corresponding to the $L\alpha$ phase (C1) and an

unknown broad peak at $q = 0.17 \text{ \AA}^{-1}$ (likely arising from excipients in the granule) were present. The intensity of the $L\alpha$ peak in the FQ/milk sample, which is known to correspond to the calcium soaps of the fatty acids liberated upon digestion of milk,¹⁸ plateaued at a relatively shorter digestion time (about 12 min, see Supporting Information, Figure S1) compared to the same peak for a sample of milk alone (about 20 min).

The structural effects were more pronounced upon the addition of FQ than addition of OZ439, despite the amphiphilic nature of OZ439,⁶ which suggests a greater degree of interaction between FQ, the milk lipids, and the lipolytic products. It was therefore anticipated, based on the structural perspective, that the amount of fatty acids released during digestion in milk would be affected by the presence of FQ and, to a lesser extent, OZ439. From the results summarized in Table S1 in the Supporting Information, which highlights the effects of the individual and combined drugs on the amount of titrated fatty acids, it was observed that the amount of titrated sodium hydroxide required during the digestion of milk was indeed affected by the addition of FQ irrespective of additional OZ439. The presence of FQ also resulted in reduced levels of titrated sodium hydroxide compared to those found with drug-free milk.

Since milk contains casein and whey proteins, liberation of amino acids and peptides by proteolytic enzymes in the pancreatin could also result in a change in pH. At pH 6.5, it was expected that the net change in pH from proteolysis would be minimal, as the carboxylic acid groups of all amino acids should be deprotonated ($pK_a \approx 2$) and the α -amines mostly protonated ($pK_a \approx 9$ –10) at this pH, resulting in no net change in pH on hydrolysis of amide bonds. Nonetheless, titrations of casein (2.5 wt%, representative of the amount of casein in bovine milk) in Tris buffer were conducted. The amount of sodium hydroxide required to neutralize the protons liberated from the digestion of casein at pH 6.5 was 0.12 ± 0.01 mmol, which amounts to $\sim 9\%$ of the total amount of titrated sodium hydroxide in digesting milk at pH 6.5. It should be noted that the casein used for the control titrations may contain residual milk fat not completely removed by the

supplier and so a portion of the titrated sodium hydroxide may still be due to lipolysis. Nevertheless, this suggests that the majority of the sodium hydroxide titrated during the digestion of milk at pH 6.5 is due to the liberation of FFAs during lipolysis and not amino acids or peptide formed by proteolysis. This is reinforced by the amounts of sodium hydroxide added in the back-titrations to pH 9.0 at the end of digestion (see Table S1, Supporting Information). For the milk-based samples approximately twice the volume titrated during the forward titration is added, but in the control digestion of casein in Tris buffer around 7 times the amount of titrant used in the initial digestion is consumed in the back-titration. This suggests that the pK_a values of the digestion products in the casein sample are on average higher than those in the milk samples, consistent with the liberation of amino acids and peptides as the major digestion products when digesting casein alone.

3.2. Solubilization of FQ during *in Vitro* Digestion of Milk (Single Drug). Readers are encouraged to refer to our previous publication for studies on solubilization of OZ439 when present alone in milk during digestion.⁶ Briefly, the solubilization of OZ439 during the digestion of milk correlated directly with the production of free fatty acids. There was a small amount of residual crystalline OZ439 in its low-solubility FB form 2 at the end of digestion; however, more than 80% of the drug was solubilized as a consequence of digestion.

3.2.1. SAXS: Behavior of FQ during Digestion in Milk. The powder scattering patterns of the crystalline FQ-FB as granules and as the “pure” API in Figure 3 showed sharp Bragg peaks

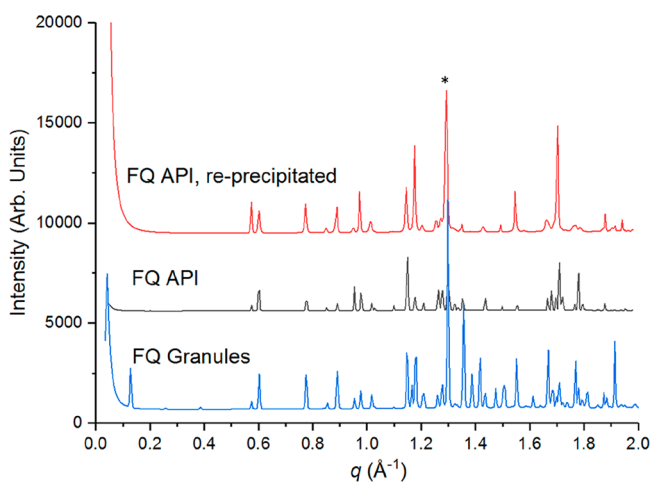


Figure 3. X-ray scattering patterns of FQ granules, FQ API, and re-precipitated FQ from the API. The asterisk denotes the characteristic diffraction peak for FQ selected for monitoring residual crystallinity during *in vitro* digestion experiments.

between $q = 0.50$ and 2.00 \AA^{-1} , with the most prominent single peak being at $q = 1.30 \text{ \AA}^{-1}$. The solubilization behavior of FQ in milk (140 mg of FQ-FB equivalent/g of milk fat) during dispersion (stirring drug in milk) and digestion was therefore monitored on the basis of the changes of the peak area with time for this characteristic FQ peak at $q = 1.30 \text{ \AA}^{-1}$.

Figure 4 shows an initially smaller peak area for FQ in milk compared to Tris buffer, which can be attributed to limited solubilization of FQ into the milk fat globules prior to digestion. A slight increase in the peak area over time was seen when FQ was dispersed and stirred in both the milk and Tris

buffer at pH 6.5 prior to the injection of lipase, which is believed to be due to re-precipitation of dissolved FQ from the gastric pre-treatment step, i.e., mixing of FQ with HCl solution. Re-precipitation of the solubilized FQ did not produce a new polymorph of the drug (Figure 3, top curve), although changes in crystal habits that resulted in identical peak positions but different relative scattering intensities and broadening of the peaks were observed.¹⁹ Prior mixing of FQ with HCl solution could favor protonation and improve the solubilization of the weakly basic FQ. When the concentration of H^+ in a system increases (i.e., lowering the pH), more drug will exist in the ionized form. The degree of ionization depends on the pH of the solution and the negative log of the drug dissociation constant (pK_a), which can be expressed by the Henderson–Hasselbalch equation.²⁰ Considering the higher pK_a values of FQ ($pK_{a1} = 8.19$ and $pK_{a2} = 6.99$)²¹ compared to OZ439 ($pK_a \approx 6.5$ – 6.7),²² more FQ would therefore exist as the ionized form at low pH.

Upon digestion of the milk formulation, the intensity of the FQ peak at $q = 1.30 \text{ \AA}^{-1}$ decreased and disappeared approximately 10 min after lipase injection (see Figure 4b). The loss of crystallinity indicates complete solubilization of FQ into the colloidal phases formed by the digested milk products via charge interactions with the liberated FA.^{17,23} Considering that less than 10% of the titrated NaOH during digestion at pH 6.5 was due to contributions from proteolysis and that most amino acids are in their zwitterionic or positively charged form at this pH, significant contributions by charged amino acids to solubilization of the drugs were not expected. It has also been shown previously that the digestion of casein by pancreatin at pH 6.5 has a negligible impact on the solid-state form of the weakly basic drug halofantrine.²⁴ Ultracentrifugation of the final (60 min) digested FQ/milk sample resulted in the formation of an upper lipid layer and an aqueous supernatant, with an insignificant amount of dense pellet phase. Hence, it can be postulated that the disappearance of the FQ peak with digestion was due to the solubilization of FQ in the lipid colloidal phases within the lipidic and aqueous layers and not precipitation of pure drug in an amorphous form. The formation of an amorphous salts of $FQ-H^+$ with ionized FAs that reside in the upper layer after ultracentrifugation is likely and will be addressed later.

3.2.2. Phase Distribution of FQ in the Digested Milk Phases: Visual Observations and Quantification Using HPLC. Visual observations of the FQ/milk samples collected at various time points after ultracentrifugation are shown in the Supporting Information, Figure S2a. Before digestion (0 min), upon ultracentrifugation, a clear aqueous supernatant with no upper lipid layer was observed, and only a separated thick yellow pellet phase was obtained, appearing to comprise lipid and yellow drug particles. This is in contrast to our previous observations upon addition of OZ439 to milk in our previous study, which resulted in distinctive lipid, aqueous, and pellet layers prior to digestion, as occurs with milk alone.⁶ The clear supernatant in the FQ samples may indicate a subtle effect of the increased density of complexes between FQ and milk components compared to that of the aqueous phase, resulting in the lipid components forming a pellet phase upon centrifugation, as opposed to the OZ439, case where they formed a creamed lipid layer. The interactions between FQ and the milk components prior to digestion did not result in the complete dissolution or amorphization of FQ, evident from the presence of the crystalline FQ peak throughout the 20 min

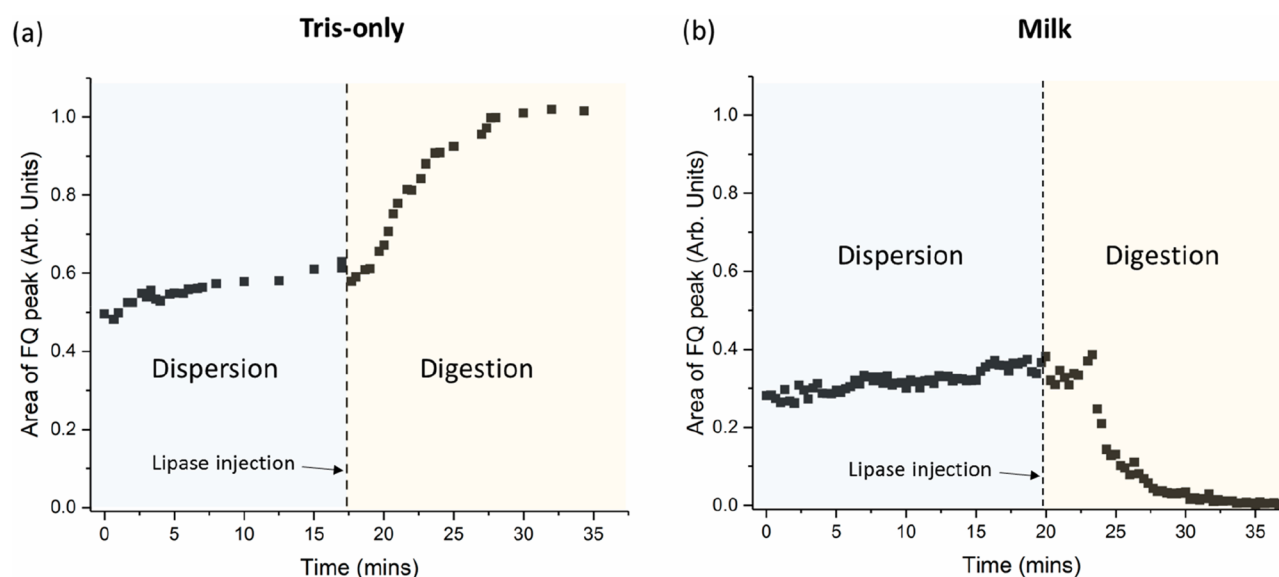


Figure 4. Changes in the area of the crystalline FQ peak at $q = 1.30 \text{ \AA}^{-1}$ in the X-ray scattering profiles in (a) Tris buffer and (b) milk during dispersion and digestion in the absence of OZ439.

(Figure 4b) and 40 min (Supporting Information, Figure S3) dispersion studies at $37 \text{ }^\circ\text{C}$.

After 2 min digestion of the FQ-containing milk dispersion, an upper lipid layer was also present after ultracentrifugation, with a progressive increase in the thickness of the upper lipid layer with time, and a subsequent decrease in the volume of the pellet phase. After 60 min of digestion, there was no observable pellet phase, and a thick upper lipid layer was observed after ultracentrifugation. Our results therefore point to the migration of FQ into the lipolytic products to the upper lipid layer as the digestion progressed due to apparent differences in densities of the initial triglycerides mixed with FQ compared to those of the corresponding digestion products containing FQ. Quantification of the amount of FQ in the partitioned phases of the digested samples using HPLC showed that the lipid layer and the aqueous supernatant layer contained about $92 \pm 6\%$ of the total FQ after 60 min digestion and most of the FQ was initially present in the pellet phase prior to lipase injection at time = 0 min (Figure 5), which agreed well with the visual observations of the samples and the SAXS results.

It was also worth noting that changes in the amount of FQ initially added to milk apparently play a role in the partitioning of FQ, as no such upper lipid phase was observed when the ratio of FQ to milk fat was doubled from 140 to 280 mg of FQ-FB equivalent/g of milk fat (see Supporting Information, Figure S4a). Thus, the differences in density appear to be at a critical point around the drug-to-fat ratios studied. Solid-state SAXS analysis of the thick pellet-only phase in the 280 mg of FQ-FB/g of milk fat sample after 60 min digestion revealed the presence of crystalline precipitates attributable to excess FQ in the digested lipids with an apparently increased density (Supporting Information, Figure S4b).

In contrast to the disappearance of the characteristic FQ peak upon digestion in milk, addition of lipase to the dispersed FQ in lipid-free Tris buffer resulted in a rapid and significant increase in the peak area (Figure 4a). FQ may exist in a supersaturated state at pH 6.5 after the gastric pre-treatment, and re-precipitation of the FQ during dispersion in the Tris buffer at the intestinal pH may not have reached equilibrium

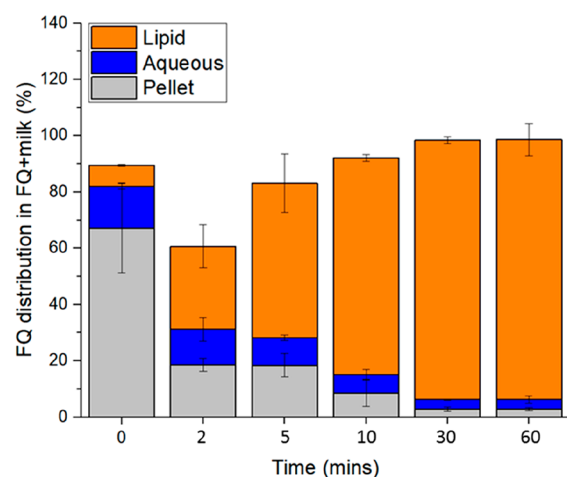


Figure 5. Distribution of FQ across the separated pellet, aqueous, and lipid layers during *in vitro* digestion of FQ in milk. The digestion reactions were terminated using 0.5 M 4-BPBA in methanol.

before digestion was initiated. Hence, addition of lipase could potentially trigger further crystallization of the FQ-FB. These observations agree well with the general consensus that the risk of drug precipitation in the small intestine is more pronounced for basic compounds in the absence of lipids and digestion, where supersaturation of the drugs could occur due to the shifts in pH from the stomach to the intestinal conditions.²⁵

3.2.3. Particle Size Distributions during Digestion of Milk Containing FQ. Solubilization of FQ in milk during digestion was also indicated from changes in the distributions of the particle sizes of milk and drug. Figure 6 shows the volume distributions of milk with and without FQ before digestion (panel a) and after 60 min digestion (panel b). Digestion of milk containing OZ439 was included for comparison. At 0 min, two populations of particle sizes were observed in the FQ/milk and the OZ439/milk samples, where in addition to the milk fat globules ($0.05\text{--}3 \mu\text{m}$), particles with size distributions between about 3 and $300\text{--}600 \mu\text{m}$ were seen due to the presence of crystalline drug particles. Larger particle

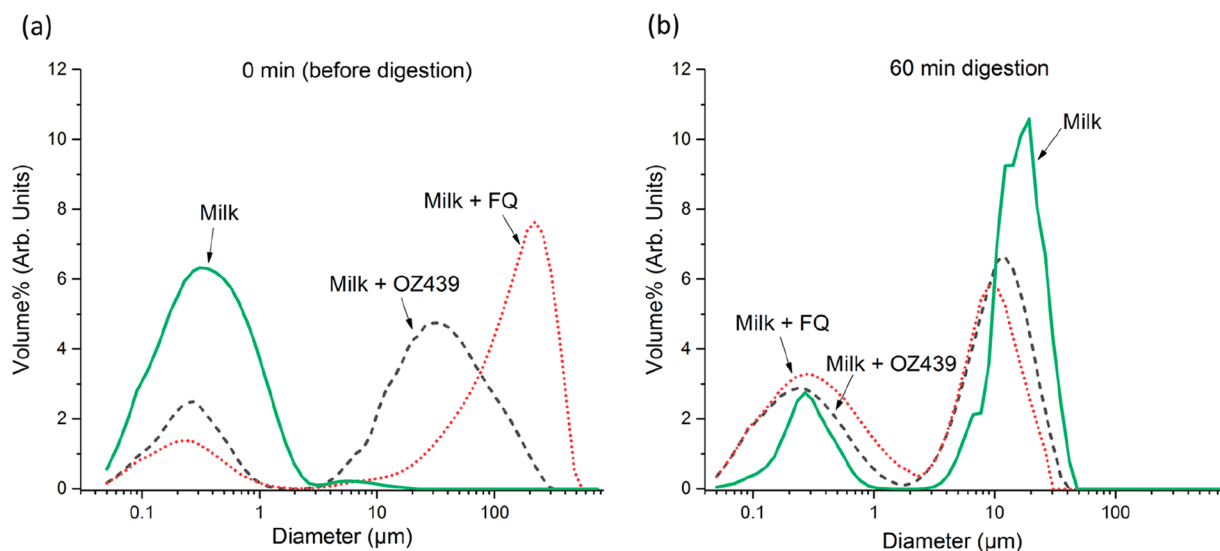


Figure 6. Particle size distributions of milk, milk containing FQ, and milk containing OZ439 (a) before digestion at 0 min and (b) after 60 min digestion.

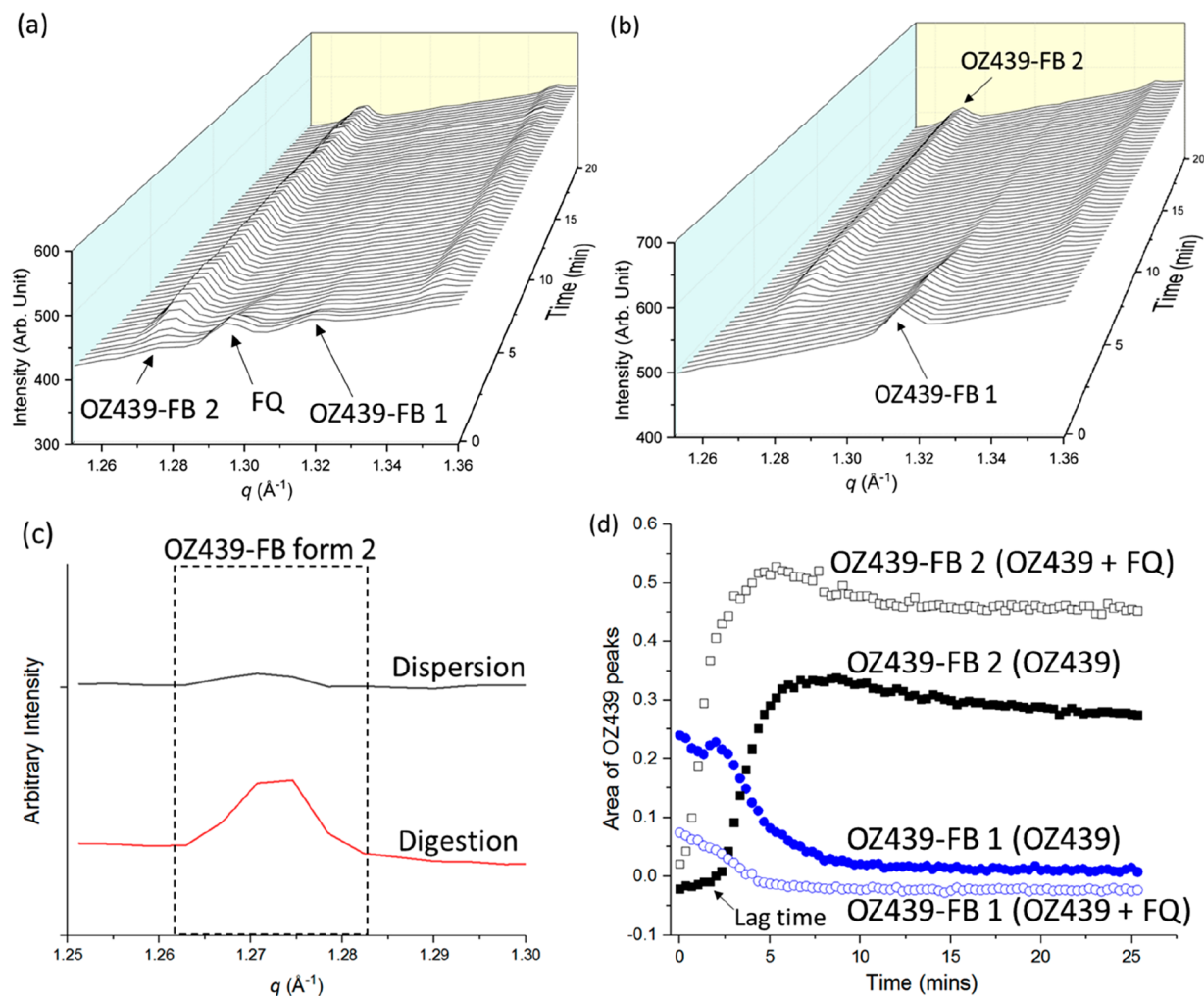


Figure 7. X-ray scattering patterns of (a) the combined OZ439 and FQ in milk during digestion and (b) OZ439 alone in milk during digestion. (c) Comparison between the OZ439-FB form 2 peaks in OZ439 + FQ after dispersion and digestion in milk at pH 6.5 and 37 $^{\circ}\text{C}$. (d) Corresponding areas of the crystalline X-ray scattering peaks from OZ439-FB form 1 and form 2 in single (OZ439 alone) and combined (OZ439 + FQ) dosage forms in milk during digestion. (Data for OZ439 alone in panels b and d are replotted from our previous study⁶ for direct comparison.)

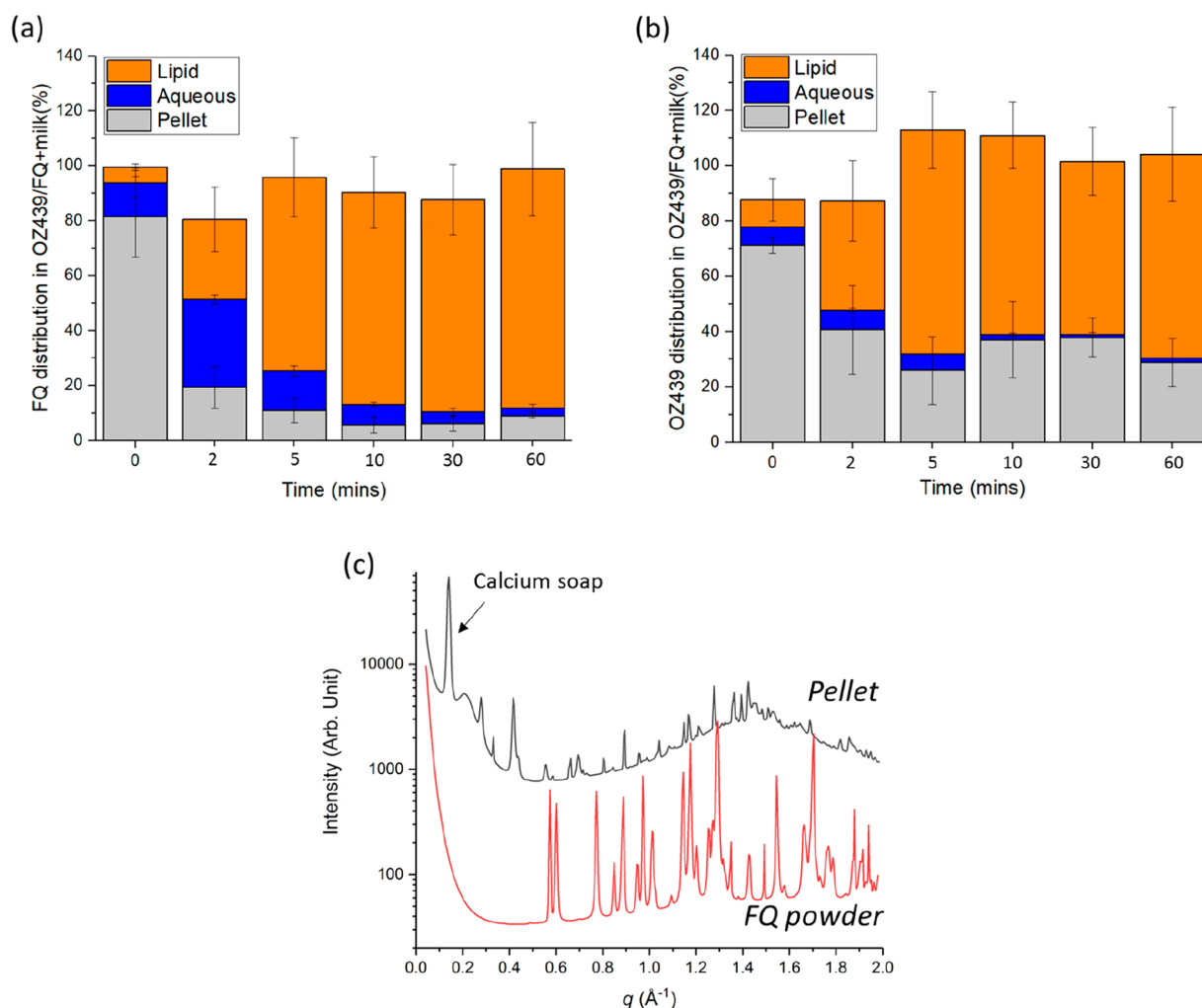


Figure 8. Distribution of (a) FQ and (b) OZ439 across the separated pellet, aqueous, and lipid layers during *in vitro* digestion of OZ439 + FQ in milk. (c) Comparison between the SAXS patterns of FQ powder and the pellet isolated after centrifugation of the digested OZ439 + FQ samples.

sizes with a greater total particle volume were observed in milk containing FQ compared with OZ439, which may be caused by aggregation of the milk fat globules. The population of these large particles shifted toward smaller diameters after digestion, with the final size distributions between 2 and 40 μm (in FQ/milk and OZ439/milk samples), which may imply solubilization of the crystalline drugs and formation of liquid crystalline colloidal particles. In contrast, digestion of milk in the absence of drugs resulted in an increase in particle sizes, with the formation of large particles between 2 and 50 μm that were correlated to the liquid crystalline phases.¹⁸ In addition, changes in the initial size distributions (0 min, Figure 6a) of the milk fat globules were also seen after the addition of OZ439 and FQ.

3.3. Solubilization of OZ439 and FQ in Combined Dosage Forms during *in Vitro* Digestion of Milk.

3.3.1. SAXS: Behavior of the Combination of OZ439 and FQ during Digestion in Milk Containing Both Drugs. Time-resolved X-ray scattering patterns (shown over a representative q range for clarity) of the combined FQ and OZ439 system during digestion in milk are shown in Figure 7a. The SAXS pattern for the digestion of OZ439 only (no FQ) in milk is also included in panel b for comparison.⁶ As was expected from the behavior of the individual drugs, disappearance of the characteristic FQ peak and polymorphic transformation of

OZ439-FB from form 1 to form 2 occurred concurrently. However, it was evident that the kinetics of formation of OZ439-FB form 2 were different than in the case of OZ439 alone, where addition of FQ induced an earlier formation of the FB form 2. The characteristic crystalline peak of the OZ439-FB form 2 was also present after 20 min of dispersion of OZ439 and FQ in milk at 37 °C and pH 6.5, as shown in Figure 7c. No crystalline OZ439-FB form 2 peak was seen during the dispersion of OZ439 in milk in the absence of FQ.⁶

Estimation of the abundances of the different polymorphs of OZ439 free base was made by integrating the area under the peaks. The results in Figure 7d show that the initial precipitation of the OZ439-FB form 2 was enhanced by the presence of FQ. The lag time for precipitation of OZ439, which was evident in the absence of FQ, was far less apparent in the presence of FQ. A greater degree of precipitation of OZ439-FB form 2 was seen throughout the digestion when FQ was co-administered, and approximately 40% more residual OZ439-FB form 2 (based on area under the peak at $q = 1.27 \text{ \AA}^{-1}$) was observed after 25 min digestion in the presence of FQ.

The following key observations can therefore be drawn on the basis of the solubilization studies obtained from the SAXS results: (1) Solubilization of OZ439 in digested milk was negatively affected by the presence of FQ. (2) Incomplete

solubilization of OZ439 was apparent after 20 min digestion. (3) Digestion of the lipids in milk was required to solubilize FQ (as seen previously for OZ439). (4) Complete disappearance of the characteristic crystalline FQ peak was observed within 20 min of digestion irrespective of the presence of OZ439.

3.3.2. Phase Distribution of OZ439 and FQ in Milk during Digestion: Quantification Using HPLC. Samples were taken at time points during the digestion of milk containing OZ439 and FQ, ultracentrifuged, and analyzed by HPLC to determine the phase distribution of the drugs. Figure 8a shows the distribution of FQ in the separated digested phases in milk when OZ439 was present as analyzed using HPLC, while Figure S2b in the Supporting Information provides a visual observation of the separated phases. Although the addition of OZ439 did not alter the general trend of the FQ distributions (i.e., more FQ in lipid layer with digestion time), the amount of FQ remaining in the pellet phase in the OZ439 + FQ system was slightly higher than in the FQ-only system, where about 10% of the total FQ resided in the pellet phase, as opposed to 3%. The presence of FQ in the pellet did not correlate directly with the results obtained from SAXS, in which the characteristic FQ peak disappeared with digestion both in the absence (Figure 4b) and in the presence of OZ439 (Figure 7a). As scattering peaks are representative of crystalline solid drug,²⁶ it was possible that the observed pellets after centrifugation were of an amorphous nature. To test this hypothesis, pellets of the digested OZ439+FQ sample at the 60 min time point were collected and analyzed using SAXS. Only crystalline peaks belonging to OZ439-FB form 2 were present in the pellet, and no crystalline FQ peaks were observed (Figure 8c). This confirmed that FQ in the pellet was in the form of an amorphous solid.

The distributions of OZ439 in the digested phases of the single OZ439 + milk system have been reported previously.⁶ Most of the OZ439 was partitioned into the upper lipid layer, and only about $12 \pm 5\%$ of the dosed drug remained the pellet phase after 60 min digestion. As shown in Figure 8b, addition of FQ reduced the solubilization of OZ439, and a significant proportion of OZ439 (about $30 \pm 9\%$ of the total OZ439) remained in the pellet phase after 60 min digestion. The results therefore support observations from the SAXS studies (Figure 7d), where the combined OZ439 + FQ dosage form exhibited larger peaks corresponding to OZ439-FB form 2 and, more importantly, correlate to the clinical bioavailability studies that indicate reduced exposure to OZ439 when it is co-administered with FQ (unpublished results).

It should be noted that the results presented in Figure 8a,b are based on the use of 0.5 M 4-BPBA as the lipase inhibitor to minimize the amount of methanol added to the system (3 μL of inhibitor in 300 μL of digested sample), as this could affect the drug distributions. As shown in Figure S2c in the Supporting Information, addition of 30 μL of methanol resulted in the disappearance of the upper lipid phase. The disappearance of the lipid phase was not caused by its solubilization into methanol, as higher concentrations of OZ439 in the aqueous supernatant phase would then be anticipated. Instead, the presence of methanol may result in changes to the relative density of the drug-containing lipid or the supernatant layers.

4. DISCUSSION

The oral bioavailability of OZ439 is significantly improved when the drug is administered after a glass of full-fat milk or a high-fat breakfast.^{4,27,28} The use of milk in pediatric populations in particular is attractive to facilitate gastrointestinal absorption of poorly water-soluble drugs, to provide essential nutrients, and to improve palatability. OZ439 is more soluble in milk than in lipid-free buffer,⁶ which is in good agreement with the increased exposure in human subjects after a high-fat meal.^{3,29} Since a combination therapy is recommended for the treatment of malaria, it is critical to understand the role of the second drug in the dosage form on the solubilization of OZ439. Ferroquine (FQ) was selected as the combination drug due to its potential to provide a single-dose therapy for malaria in concert with OZ439, and clinical trials of combined OZ439 and FQ treatments are in progress.¹³ These trials have revealed a decreased exposure to OZ439 when co-formulated with FQ in milk powder, hypothesized to be due to decreased solubilization of OZ439 during digestion.

Herein, we demonstrated that the solubilization behavior of OZ439 in milk during digestion was indeed negatively affected by FQ. Crystallization of the FB form 2 polymorph of OZ439 from the FB form 2 polymorph in FQ-free milk was enhanced by digestion driving the transformation.⁶ In contrast, the presence of FQ triggered the formation of OZ439-FB form 2 even prior to digestion and accelerated its precipitation during digestion, which reduced the overall solubilization of OZ439 in milk. The mechanism by which FQ enhanced the crystallization of OZ439 in its less soluble FB form 2 polymorph is not understood, as crystallization is a complex process and the solid-state transformation of a drug can be governed by thermodynamic (stability of a polymorph and the tendency to transform to another polymorph) and kinetic (how fast the transformation reached equilibrium) processes,³⁰ which are more complicated and prone to the influence of other components in a multi-drug environment.³¹ A possibility is that the solubilization of FQ in the fat globules prior to digestion (Figure 4a) may reduce the initial solubilization of OZ439 in the same globules, increasing the amount of supersaturated free drug in solution, hence enhancing the likelihood of nucleation and crystal growth of the OZ439-FB form 2. Excipients in the FQ granules may also form pre-nucleation aggregates and act as a template to promote the nucleation of OZ439.

Ferroquine has an apparently strong affinity to the fatty acids liberated during milk digestion (evidenced by the lower consumption of NaOH during forward titration of FQ in milk and substantial changes to the self-assembled liquid crystalline structures). It is likely, therefore, that it competes for the fatty acids more strongly in this respect than OZ439, reducing the capacity for additional solubilization of OZ439 into the digested lipids. The reduction in the amount of sodium hydroxide titrated in both the forward and back-titrations when FQ is present in milk (see Supporting Information, Table S1) suggests that FQ may also have an inhibitory effect on the digestive enzymes in pancreatin, resulting in lower extents of digestion. Previous studies have shown that, in amorphous solid dispersion systems, the concentrations of anti-HIV drugs in solution can vary, depending on the partner drug and the presence of excipients.³² To look at this a different way, the desire for ion-pairing of both weakly basic drugs with oleic acid may also induce a common ion effect,

reducing the solubility of both drugs in the digested fat droplet. Although usually recognized as an aqueous phenomenon, this effect could be anticipated, although the solubility of FQ is apparently high even in the presence of OZ439 but the converse is not true. As the solubility product is likely different with different fatty acids, this concept may even provide a handle for future formulation efforts with such systems by selection or addition of specific triglycerides to liberate fatty acids to manipulate the magnitude of the effect.

As discussed, the presence of OZ439 does not lead to precipitation of FQ upon digestion, evidenced by a lack of crystalline precipitates of FQ in both the single-drug (FQ in milk) and the combined (OZ439 + FQ in milk) systems due to the formation of amorphous pellets. Conversion of drugs from the crystalline state to the amorphous state upon digestion has been typically observed for basic drugs that are ionized at the digesting pH in lipid-based formulations. Examples of such drugs are cinnarizine ($pK_a = 7.5$) and carvedilol ($pK_a = 7.8$), which can interact with the carboxylic acid group of the fatty acids.^{17,23,33,34} As the amorphous solids can potentially undergo fast re-dissolution,³³ it is therefore speculated that the presence of FQ in the pellet in the combined drug system would not largely affect the *in vivo* absorption due to the promotion of supersaturated solution with higher thermodynamic activity (compared to the crystal counterpart) upon the drug dissolution.^{35,36}

While milk as a drug delivery vehicle is problematic from a regulatory standpoint, it is useful to understand the impact of substituting milk with highly regulated milk powder or infant formula as a possible excipient in a dry powder formulation. More control over drug-to-fat ratios and potential for selection of systems with alternative lipid compositions to tune the interactions of the drug with the digesting lipid systems would be added benefits of such an approach that will be further investigated using these new approaches to study drug solubilization and solid-state behavior in future studies.

5. CONCLUSIONS

Milk can be used to enhance the solubilization of OZ439 and FQ during *in vitro* lipolysis under intestinal conditions. The overall solubilization of OZ439 during digestion was, however, reduced by the presence of FQ when co-formulated in milk. Interaction between FQ-H⁺ and the liberated ionized fatty acids led to the formation of amorphous solids, while OZ439 precipitated predominantly as the stable form 2 polymorph of the crystalline free base. Addition of FQ at a critical level influenced the colloidal stability of the milk fat globules and resulted in aggregation of the lipid particles. Stronger interaction between FQ and the milk lipids compared to that of OZ439 was also reflected by the significant changes in the type of colloidal structures formed by the self-assembly of milk lipolytic products. Tuning these interactions through selection of alternative milk-like lipid systems or drug-to-fat ratios using powdered systems could provide enhanced solubilization and absorption of this life-saving drug combination.

■ ASSOCIATED CONTENT

📄 Supporting Information

The Supporting Information is available free of charge on the ACS Publications website at DOI: 10.1021/acs.molpharmaceut.8b01333.

Changes in intensity of diffraction peak for FQ during digestion of milk using FQ granules; table of titrated volume of sodium hydroxide solution during digestion for each system studied; images of digested material after ultracentrifugation; changes in intensity of diffraction peak for FQ during dispersion in milk (PDF)

■ AUTHOR INFORMATION

Corresponding Author

*Telephone: +61 3 99039112. Fax: +61 3 99039583. E-mail: ben.boyd@monash.edu.

ORCID

Andrew J. Clulow: 0000-0003-2037-853X

Ben J. Boyd: 0000-0001-5434-590X

Notes

The authors declare the following competing financial interest(s): Dr. Hanu Ramachandruni is an employee of Medicines for Malaria Venture, which owns the OZ439 candidate, and Stephane Beilles is an employee of Sanofi, which owns ferroquine.

■ ACKNOWLEDGMENTS

This work was funded by the Bill and Melinda Gates Foundation grant number OPP1160404 in collaboration with Medicines for Malaria Venture (MMV). Funding is also acknowledged from the Australian Research Council under the Discovery Projects scheme DP160102906. The SAXS experiments for this work were conducted on the SAXS/WAXS beamline of the Australian Synchrotron, part of ANSTO. The authors thank Dr. Niya Bowers for technical and historical discussions around co-administration of OZ439 and FQ with milk.

■ REFERENCES

- (1) Porter, C. J. H.; Charman, W. N., Oral lipid-based formulations: using preclinical data to dictate formulation strategies for poorly water-soluble drugs. In *Oral lipid-based formulations: enhancing the bioavailability of poorly water-soluble drugs*, Hauss, D. J., Ed.; CRC Press: 2007; Vol. 170, p 185.
- (2) Persson, E. M.; Gustafsson, A. S.; Carlsson, A. S.; Nilsson, R. G.; Knutson, L.; Forsell, P.; Hanisch, G.; Lennernas, H.; Abrahamsson, B. The effects of food on the dissolution of poorly soluble drugs in human and in model small intestinal fluids. *Pharm. Res.* **2005**, *22* (12), 2141–51.
- (3) Healthy Volunteer Study of the Pharmacokinetics of Oral Piperazine With OZ439 + TPGS Formulation in the Fasted State, <https://clinicaltrials.gov/ct2/show/study/NCT01853475>, accessed February 27, 2019.
- (4) Darpo, B.; Ferber, G.; Siegl, P.; Laurijssens, B.; Macintyre, F.; Toovey, S.; Duparc, S. Evaluation of the QT effect of a combination of piperazine and a novel anti-malarial drug candidate OZ439, for the treatment of uncomplicated malaria. *Br. J. Clin. Pharmacol.* **2015**, *80* (4), 706–715.
- (5) Boyd, B. J.; Salim, M.; Clulow, A. J.; Ramirez, G.; Pham, A.; Hawley, A. The impact of digestion is essential to the understanding of milk as a drug delivery system for poorly water soluble drugs. *J. Controlled Release* **2018**, *292*, 13–17.
- (6) Salim, M.; Khan, J.; Ramirez, G.; Clulow, A. J.; Hawley, A.; Ramachandruni, H.; Boyd, B. J. Interactions of Artefenomel (OZ439) with Milk during Digestion: Insights into Digestion-Driven Solubilization and Polymorphic Transformations. *Mol. Pharmaceutics* **2018**, *15* (8), 3535–3544.
- (7) Clulow, A. J.; Salim, M.; Hawley, A.; Gilbert, E. P.; Boyd, B. The curious case of the OZ439 mesylate salt - an amphiphilic antimalarial

drug with diverse solution and solid state structures. *Mol. Pharmaceutics* **2018**, *15* (5), 2027–2035.

(8) McCarthy, J. S.; Baker, M.; O'Rourke, P.; Marquart, L.; Griffin, P.; Hooft van Huijsduijnen, R.; Möhrle, J. J. Efficacy of OZ439 (artefenomel) against early *Plasmodium falciparum* blood-stage malaria infection in healthy volunteers. *J. Antimicrob. Chemother.* **2016**, *71* (9), 2620–2627.

(9) White, N. Antimalarial drug resistance and combination chemotherapy. *Philos. Trans. R. Soc. London B. Biol. Sci.* **1999**, *354* (1384), 739–49.

(10) Biot, C.; Chavain, N.; Dubar, F.; Pradines, B.; Trivelli, X.; Brocard, J.; Forfar, I.; Dive, D. Structure–activity relationships of 4-N-substituted ferroquine analogues: Time to re-evaluate the mechanism of action of ferroquine. *J. Organomet. Chem.* **2009**, *694* (6), 845–854.

(11) Charman, S. A.; Arbe-Barnes, S.; Bathurst, I. C.; Brun, R.; Campbell, M.; Charman, W. N.; Chiu, F. C. K.; Chollet, J.; Craft, J. C.; Creek, D. J.; Dong, Y.; Matile, H.; Maurer, M.; Morizzi, J.; Nguyen, T.; Papastogiannidis, P.; Scheurer, C.; Shackelford, D. M.; Sriraghavan, K.; Stingelin, L.; Tang, Y.; Urwyler, H.; Wang, X.; White, K. L.; Wittlin, S.; Zhou, L.; Vennerstrom, J. L. Synthetic ozonide drug candidate OZ439 offers new hope for a single-dose cure of uncomplicated malaria. *Proc. Natl. Acad. Sci. U. S. A.* **2011**, *108* (11), 4400–4405.

(12) Chavain, N.; Vezin, H.; Dive, D.; Touati, N.; Paul, J.-F.; Buisine, E.; Biot, C. Investigation of the Redox Behavior of Ferroquine, a New Antimalarial. *Mol. Pharmaceutics* **2008**, *5* (5), 710–716.

(13) To Evaluate the Efficacy of a Single Dose Regimen of Ferroquine and Artefenomel in Adults and Children With Uncomplicated *Plasmodium falciparum* Malaria (FALCI), <https://clinicaltrials.gov/ct2/show/NCT02497612>, accessed February 27, 2019.

(14) Khan, J.; Hawley, A.; Rades, T.; Boyd, B. J. In Situ Lipolysis and Synchrotron Small-Angle X-ray Scattering for the Direct Determination of the Precipitation and Solid-State Form of a Poorly Water-Soluble Drug During Digestion of a Lipid-Based Formulation. *J. Pharm. Sci.* **2016**, *105*, 2631–2639.

(15) Boetker, J. P.; Rantanen, J.; Arnfast, L.; Doreth, M.; Rajjada, D.; Loebmann, K.; Madsen, C.; Khan, J.; Rades, T.; Mullertz, A.; Hawley, A.; Thomas, D.; Boyd, B. J. Anhydrate to hydrate solid-state transformations of carbamazepine and nitrofurantoin in biorelevant media studied in situ using time-resolved synchrotron X-ray diffraction. *Eur. J. Pharm. Biopharm.* **2016**, *100*, 119–27.

(16) Kirby, N. M.; Mudie, S. T.; Hawley, A. M.; Cookson, D. J.; Mertens, H. D. T.; Cowieson, N.; Samardzic-Boban, V. A low-background-intensity focusing small-angle X-ray scattering undulator beamline. *J. Appl. Crystallogr.* **2013**, *46* (6), 1670–1680.

(17) Khan, J.; Rades, T.; Boyd, B. J. Lipid-Based Formulations Can Enable the Model Poorly Water-Soluble Weakly Basic Drug Cinnarizine To Precipitate in an Amorphous-Salt Form During In Vitro Digestion. *Mol. Pharmaceutics* **2016**, *13* (11), 3783–3793.

(18) Clulow, A. J.; Salim, M.; Hawley, A.; Boyd, B. J. A closer look at the behaviour of milk lipids during digestion. *Chem. Phys. Lipids* **2018**, *211*, 107–116.

(19) Inoue, M.; Hirasawa, I. The relationship between crystal morphology and XRD peak intensity on CaSO₄·2H₂O. *J. Cryst. Growth* **2013**, *380*, 169–175.

(20) Physicochemical properties of drugs in solution. In *Physicochemical principles of pharmacy*, 2nd ed.; Florence, A. T., Attwood, D., Eds.; Macmillan Press: London, 1988; p 63.

(21) Biot, C.; Dive, D., Bioorganometallic chemistry and malaria. In *Medicinal Organometallic Chemistry*; Jaouen, G., Metzler-Nolte, N., Eds.; Springer: Heidelberg, 2010; Vol. 32, p 155.

(22) Dong, Y.; Wang, X.; Kamaraj, S.; Bulbule, V. J.; Chiu, F. C. K.; Chollet, J.; Dhanasekaran, M.; Hein, C. D.; Papastogiannidis, P.; Morizzi, J.; Shackelford, D. M.; Barker, H.; Ryan, E.; Scheurer, C.; Tang, Y.; Zhao, Q.; Zhou, L.; White, K. L.; Urwyler, H.; Charman, W. N.; Matile, H.; Wittlin, S.; Charman, S. A.; Vennerstrom, J. L.

Structure–Activity Relationship of the Antimalarial Ozonide Artefenomel (OZ439). *J. Med. Chem.* **2017**, *60* (7), 2654–2668.

(23) Stillhart, C.; Dürr, D.; Kuentz, M. Toward an Improved Understanding of the Precipitation Behavior of Weakly Basic Drugs from Oral Lipid-Based Formulations. *J. Pharm. Sci.* **2014**, *103* (4), 1194–1203.

(24) Boyd, B. J.; Salim, M.; Clulow, A. J.; Ramirez, G.; Pham, A. C.; Hawley, A. The impact of digestion is essential to the understanding of milk as a drug delivery system for poorly water soluble drugs. *J. Controlled Release* **2018**, *292*, 13–17.

(25) Stillhart, C.; Kuentz, M. Trends in the Assessment of Drug Supersaturation and Precipitation In Vitro Using Lipid-Based Delivery Systems. *J. Pharm. Sci.* **2016**, *105* (9), 2468–76.

(26) Newman, A. W.; Byrn, S. R. Solid-state analysis of the active pharmaceutical ingredient in drug products. *Drug Discovery Today* **2003**, *8* (19), 898–905.

(27) A Dose-escalation Study to Investigate Safety and Toleration of OZ439, <https://clinicaltrials.gov/ct2/show/study/NCT01713608>, accessed February 27, 2019.

(28) Phyo, A. P.; Jittamala, P.; Nosten, F. H.; Pukrittayakamee, S.; Imwong, M.; White, N. J.; Duparc, S.; Macintyre, F.; Baker, M.; Möhrle, J. J. Antimalarial activity of artefenomel (OZ439), a novel synthetic antimalarial endoperoxide, in patients with *Plasmodium falciparum* and *Plasmodium vivax* malaria: an open-label phase 2 trial. *Lancet Infect. Dis.* **2016**, *16* (1), 61–69.

(29) Study To Investigate The Relative Bioavailability of OZ439 Formulations In Healthy Volunteers, <https://clinicaltrials.gov/ct2/show/NCT01383096>, accessed February 27, 2019.

(30) Bryn, S. R.; Zografi, G.; Chen, X. *Solid-state properties of pharmaceutical materials*; John Wiley & Sons, Inc.: 2017.

(31) Trasi, N. S.; Taylor, L. S. Thermodynamics of Highly Supersaturated Aqueous Solutions of Poorly Water-Soluble Drugs—Impact of a Second Drug on the Solution Phase Behavior and Implications for Combination Products. *J. Pharm. Sci.* **2015**, *104* (8), 2583–93.

(32) Arca, H. Ç.; Mosquera-Giraldo, L. I.; Dahal, D.; Taylor, L. S.; Edgar, K. J. Multidrug, Anti-HIV Amorphous Solid Dispersions: Nature and Mechanisms of Impacts of Drugs on Each Other's Solution Concentrations. *Mol. Pharmaceutics* **2017**, *14* (11), 3617–3627.

(33) Sassene, P. J.; Knopp, M. M.; Hesselkilde, J. Z.; Koradia, V.; Larsen, A.; Rades, T.; Müllertz, A. Precipitation of a poorly soluble model drug during in vitro lipolysis: Characterization and dissolution of the precipitate. *J. Pharm. Sci.* **2010**, *99* (12), 4982–4991.

(34) Mistic, Z.; Jung, D. Š.; Sydow, G.; Kuentz, M. Understanding the interactions of oleic acid with basic drugs in solid lipids on different biopharmaceutical levels. *J. Excip. Food. Chem.* **2014**, *5* (2), 113.

(35) Michaelsen, M. H.; Wasan, K. M.; Sivak, O.; Müllertz, A.; Rades, T. The Effect of Digestion and Drug Load on Halofantrine Absorption from Self-nanoemulsifying Drug Delivery System (SNEDDS). *AAPS J.* **2016**, *18* (1), 180–186.

(36) Thomas, N.; Holm, R.; Müllertz, A.; Rades, T. In vitro and in vivo performance of novel supersaturated self-nanoemulsifying drug delivery systems (super-SNEDDS). *J. Controlled Release* **2012**, *160* (1), 25–32.